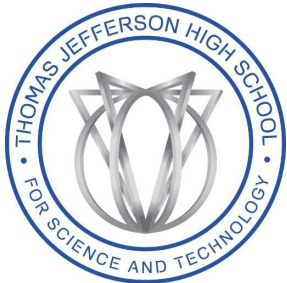# Development of Python-based Toolkit to Improve Analysis of Atom Probe Tomography Data

Vishal Kanigicherla

Science and Technology Department, Thomas Jefferson High School for Science and Technology, Alexandria, VA, USA

Atom Probe Tomography

- Atom-by-atom dissection of a material volume
- Sub-nanometer resolution, and chemical sensitivities approaching 10 atomic ppm
- Breakdown by field evaporation
- Time-of-flight mass spectrometry and impact recordings create reconstruction
- Mass-to-charge ratio and (x, y, z) recorded in POS file
- Proximity histogram (proxigram) details at% composition of thin ~.1 nm shells of sample about predetermined surface
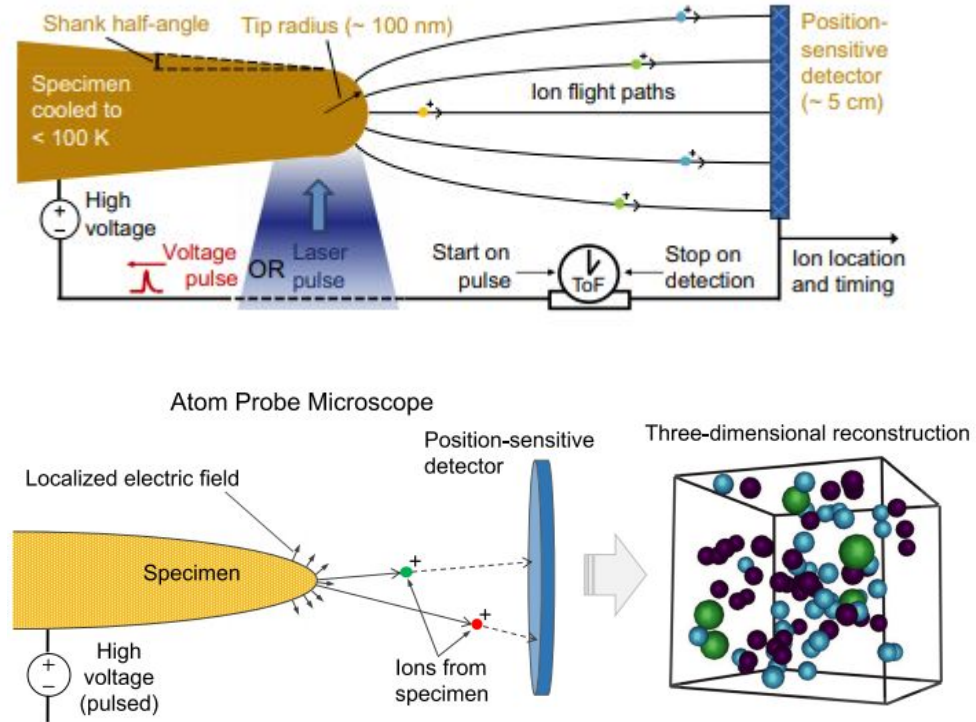

Figure 1. The schematics above represent the process of atom probe tomography, and demonstrate how reconstructions can be developed from a position-sensitive detector. Image sourced from Reddy, S. M., Saxey, D. W., Rickard, W. D. A., Fougerouse, D., Montalvo, S. D., Verberne, R., & van Riessen, A. (2020).

Literature Review - The Challenges of Atom Probe Tomography

- Leaves molecular artifacts in sample through FIB milling and other processing (Tamura, M., Shukuri, S., Moniwa, M., & Default, M. (1986))
- Isotopic overlaps left inherent to time-of-flight mass spectrometry
- Mass spectrum ranging and peak identification is difficult
- Maximum separation algorithm heavily dependent on user-input parameters, could use optimization (Vincent, G. B., Proudian, A. P., & Zimmerman, J. D. (2020))
- Lack of algorithms to calculate error statistics and relevant thermodynamic quantities such as Gibbs interfacial excess of solute for which APT is easily applicable (Hellman, O. C., & Seidman, D. N. (2002), Krakauer, B. W., & Seidman, D. N. (1993))
- Large amounts of data make processing generally tedious - optimization and automation of the process is a viable direction for development

Project Direction

- This project seeks to holistically address APT data analysis using Python, liberating APT data analysis from proprietary software while also improving existing data analysis techniques by implementing various algorithms employing optimization and machine learning. This project is trying to test the extent to which established techniques are user-friendly, accessible, and optimized.

Gibbsian Interfacial Excess of Solute

$$\Gamma_s = \left(\sum_{n=1}^{N} \frac{(C_n - C_0)}{A_n} \right) / (1 - C_0)$$

$$A_i = \frac{N_i}{\rho \Delta l}$$

- Γs, concentration of solute within an infinitesimally small interface, a "Gibbs dividing surface," between two bulk phases of a material
- Atom probe proxigram data is very well suited for this calculation, already binned shells
- Prior formulations require knowledge of area of shell thickness, possible to bypass
- Circumvented *a priori* requisites for ρ using lattice parameter of molecular species and assumption of Bravais crystal lattice structure

Figure 2. Hellman & Seidman (2002) determined the above formulations that eliminated the need for *a priori* knowledge of slice area, and through dimensional analysis substituted a formula

Manipulation of Proxigram .csv and Raw Data .pos and .epos Files

- .pos files are binary files including x, y, z position data and mass-to-charge ratio
- .epos files are extended .pos files with 11 attributes instead of 4
- Proxigrams are .csv files which note atom counts of individual species in ~.1 nm shells shells at specific proximities from an interface

Distance (nm)	Fe %	Fe % Err	Ni %	Ni % Err	Mn %	Mn % Err
-4.9	75.16451787795387	0.05445965444524276	13.865768674905677	0.043560415349015134	6.2409473431495535	0.030490462361572823
-4.7	75.1562772001456	0.054340402552356025	13.928057098545633	0.043541958204319796	6.2110493915080145	0.030352202698738763
-4.5	75.07361105171545	0.05442287289575195	13.976200545173187	0.0436226454202262	6.177309581395054	0.0302873831576798
-4.3	75.1330377294043	0.05458926806809757	13.958028072796454	0.04376708684280058	6.206405603067131	0.030471027304262124
-4.1	75.12475615841764	0.055003939136313025	13.933642685400612	0.04406234712815362	6.2716703067381285	0.0308493224984128

Figure 3. Modified proxigram at% .csv file including spatial error calculations for plotting proxigram profile.

Distance (nm)	Rn % (27Da)	Fe %	Mn %	Cr %	C %	Ni %	Al %	Cu %	NiH %	C2 %	C3 %	C4 %	Ca %	Ga %	H %	Sample Count
-4.949999809	120248	865188	270480	85353	32141	91196	61543	28948	0	0	0	0	242	211	141	1555691

Figure 4. Unmodified proxigram of atom counts. Note Rn % (27Da), raw data for the 27 Dalton which could be $27Al^{1+}$, $54Fe^{2+}$, or $54Cr^{2+}$. This ambiguity of isotopic overlap requires further resolution, one of the tasks executed by the toolkit.

Programs and Dependencies

Python code was written in order to:

- Take user-input for manual peak decomposition in proxigrams.
- Convert proxigram atom counts to at.% values.
- Generate profiles of proxigram data after discarding irrelevant isotopes.
- Create core compositions from user identification of matrix and precipitate of profile.
- Turn large POS files into workable CSVs.
- Calculate and compositional error statistics for proxigram and CSV.
- Take inputs for calculating average radius, vol fraction, and number density, do the calculation, and report the uncertainty.
- Generate a mass spectrum graph and analysis from POS CSV.
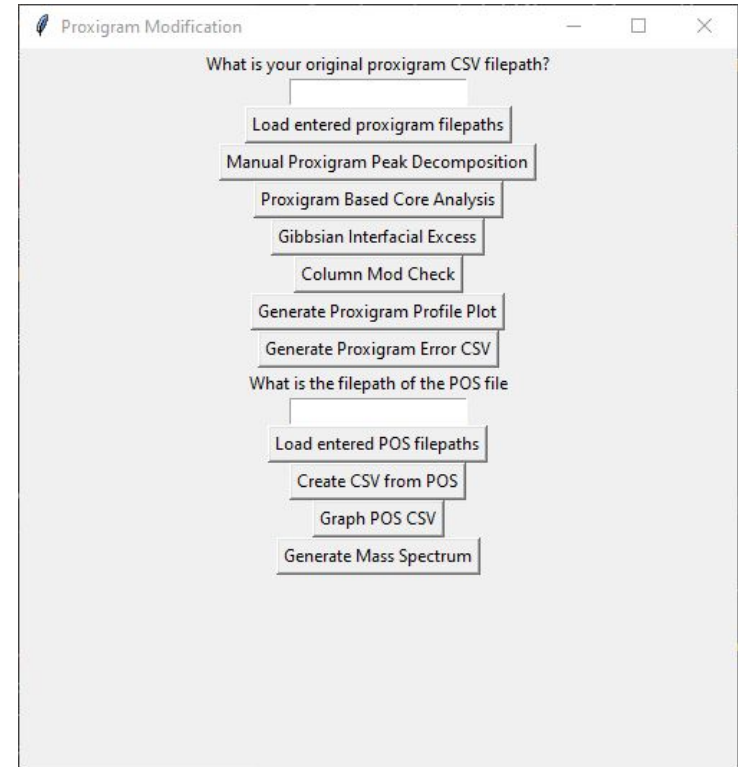- Consolidate programs into GUI using Py2App and tkinter for better user experience.

Figure 5. Image of user interface application with integrated programs. Packages used in this project and thus system requirements are *struct*, *pandas*, *tkinter*, *numpy*, *sklearn*, and *matplotlib*.
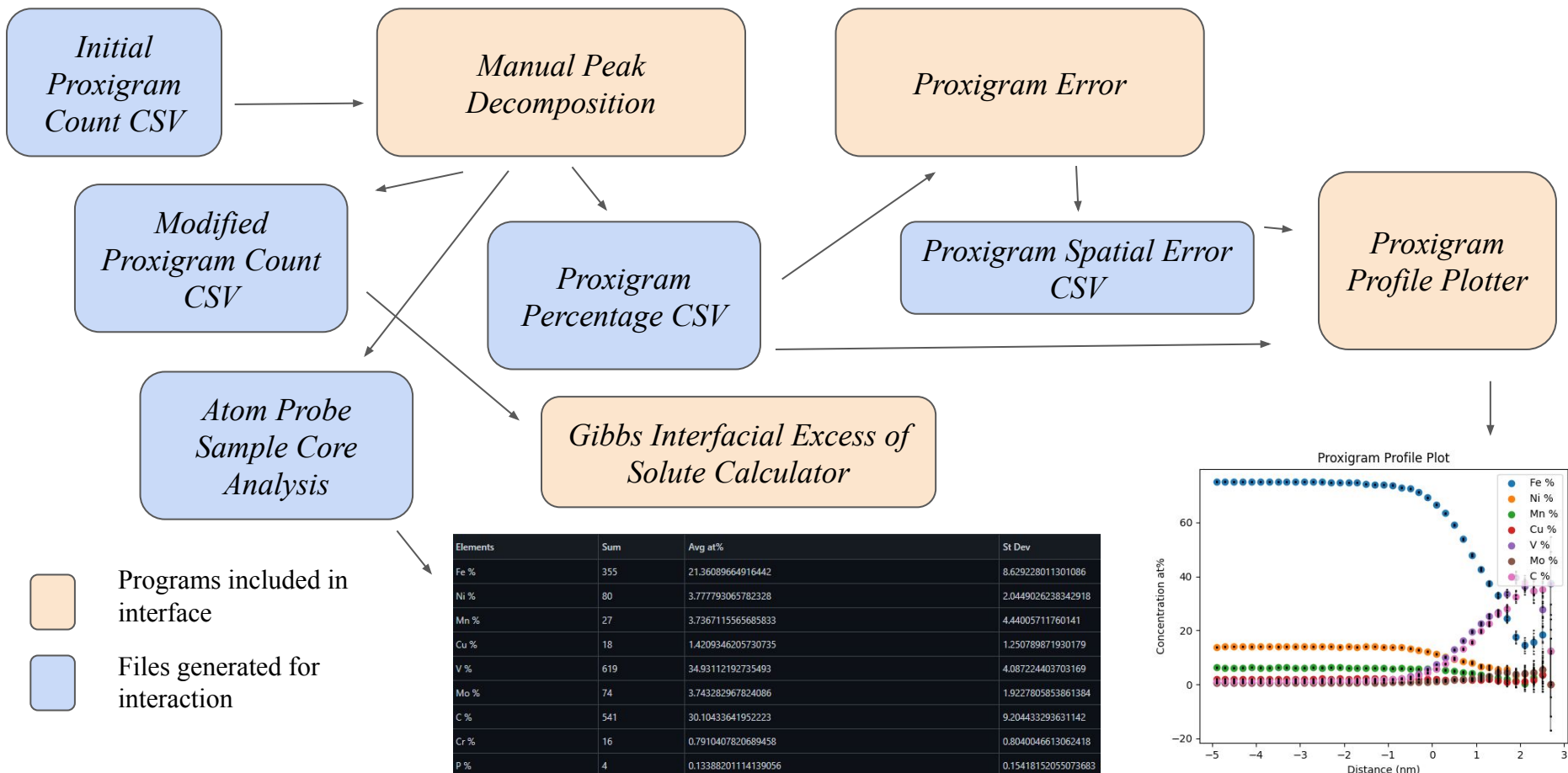
Initial Proxigram Count CSV

Manual Peak Decomposition

Proxigram Error

Modified Proxigram Count CSV

Proxigram Percentage CSV

Proxigram Spatial Error CSV

Proxigram Profile Plotter

Atom Probe Sample Core Analysis

Gibbs Interfacial Excess of Solute Calculator

Programs included in interface

Files generated for interaction

Elements	Sum	Avg at%	St Dev
Fe %	355	21.36089664916442	8.629228011301086
Ni %	80	3.777793065782328	2.0449026238342918
Mn %	27	3.73671155565685833	4.44005711760141
Cu %	18	1.4209346205730735	1.250789871930179
V %	619	34.93112192735493	4.087224403703169
Mo %	74	3.743282967824086	1.9227805853861384
C %	541	30.10433641952223	9.204433293631142
Cr %	16	0.7910407820689458	0.8040046613062418
P %	4	0.13388201114139056	0.15418152055073683

Proxigram Profile Plot

Fe %
Ni %
Mn %
Cu %
V %
Mo %
C %

Concentration at%

Distance (nm)

Figure 6. Programs written to interact with proxigram data
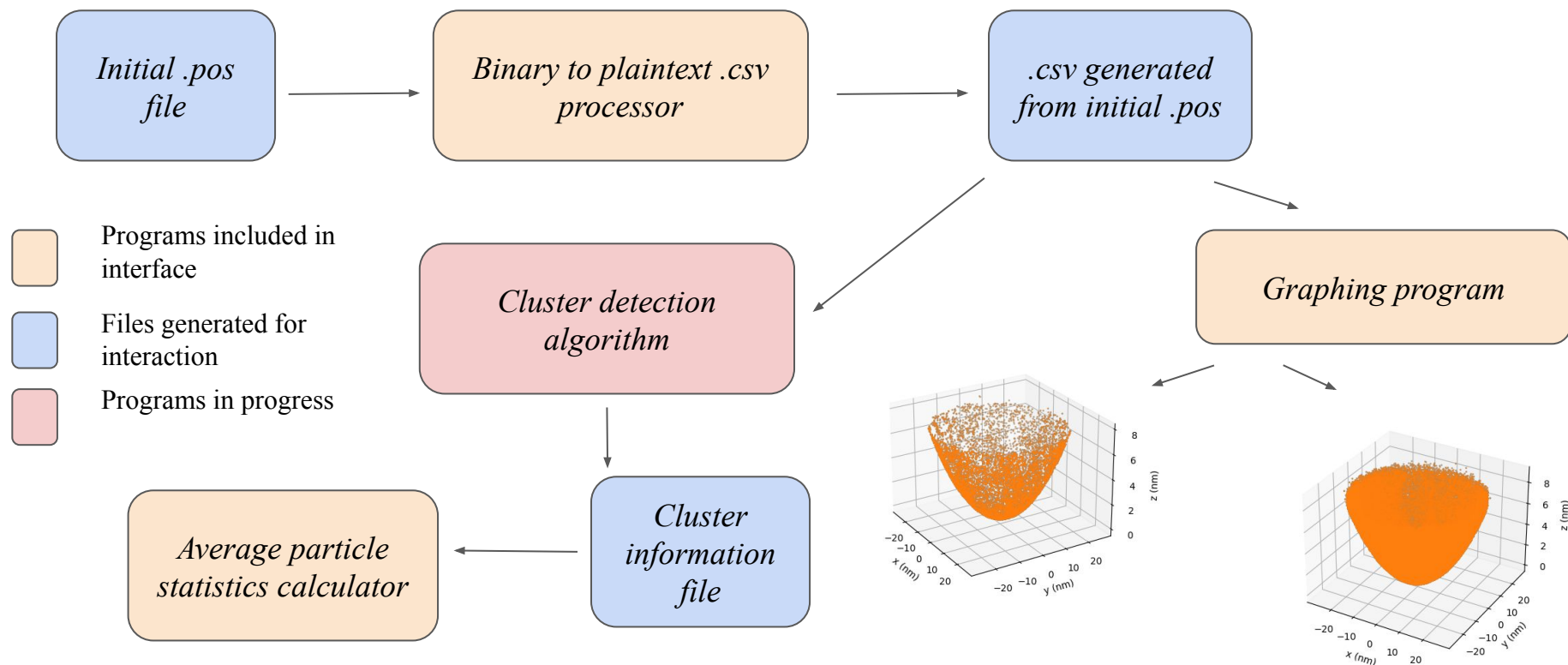
Figure 7. Programs written to interact with initial raw .pos and .epos data. A major bottleneck with interaction with .pos files is the large amounts of data, often totaling hundreds of millions of atoms to parse. Therefore, optimization and implementation of SQL along with more algorithms are a high priority to moving forward in work on .pos files. The graph is a sample of 10,000 and 100,000 atoms in a sample APT run.

Cluster Analysis and Detection


```
Data columns (total 5 columns):
 #   Column      Non-Null Count  Dtype
---  ------      --------------  -----
 0   Unnamed: 0  90000 non-null  int64
 1   0           90000 non-null  float64
 2   1           90000 non-null  float64
 3   2           90000 non-null  float64
 4   3           90000 non-null  float64
dtypes: float64(4), int64(1)
memory usage: 3.4 MB
[0 0 0 ... 0 0 0]
Counter({0: 89602, -1: 224, 4: 30, 1: 24, 3: 24, 2: 18, 10: 17, 6: 13, 11: 10, 5: 10, 8: 8, 7: 8, 9: 6, 12: 6})
Number of Clusters = 13
PS C:\Git\apt-csv-work>
```
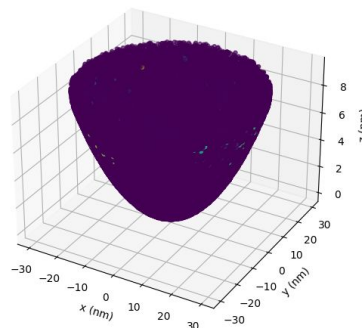
- Cameca Integrated Analysis and Visualiztion Software (IVAS), a commonly used commercial software for APT data analysis, has the ability to output a dataset of an atom probe sample with cluster counts of certain isotopes in isoconcentration surfaces defined by user
- Clips clusters of needle dataset, export two times (clipped and bounded)
- Approximate clusters as spheres, calculate equivalent radius, volume, st. dev, and number density
- Cluster detection:
  - IVAS outputs sometimes under/over estimates cluster counts
  - DBSCAN as alternative to compare with
    - In progress, currently just skeleton

Figure 8. 90000 data point cluster search run. 13 clusters detected. Visualization on left, need to remove noise (purple).

Results

- The main application interface and related programs can be found at https://github.com/sakanak/apt-csv-work
- Current algorithms in the application are those written expressly for the sake of automation of manual tasks, with the exception of the calculation software for the Gibbs interfacial excess of solute and the POS interactions
- All programs were checked to have complete accuracy through comparison with past files available at the Naval Research Laboratory
- The formulation used for Gibbs interfacial excess relies on estimations made for number density using an assumed lattice parameter and structure - further development could reduce such error as proposed in Krakauer & Seidman et al. (1993) for an APFIM TEM calculation of Gibbsian excess

Conclusions

- Confirmation of the ability of toolkit to automate analysis of data in APT
- Implementation of calculators for specific thermodynamic quantities
- Identifiable room for development in areas dealing with large amounts of data through implementation of optimization algorithms and different data structures

Further Perspectives

- A few tasks for the toolkit currently in development include:
  - Optimizing cluster detection
  - Executing peak detection and automatic ranging and isotope assignment using available isotope abundances table
  - Modelling matrix composition to track precipitation as a function of time
  - Additional tasks are to be determined
- Further implementation of different techniques; one example includes utilizing Ripley's K-function and machine learning to optimize the maximum separation algorithm for cluster detection, while another involves optimizing existing simulations for field evaporation such as TAPSim

Acknowledgements

References

(1)   Reddy, S. M., Saxey, D. W., Rickard, W. D. A., Fougerouse, D., Montalvo, S. D., Verberne, R., & van Riessen, A. (2020). *GGR Cutting‑Edge Review Atom Probe Tomography: Development and Application to the Geosciences. Geostandards and Geoanalytical Research.* doi:10.1111/ggr.12313

(2)   Lefebvre-Ulrikson, W., Vurpillot, F. & Sauvage, X. (2016). *Atom Probe Tomography*. London: Academic Press.

(3)   Kelly, T. F., & Miller, M. K. (2007). *Atom probe tomography. Review of Scientific Instruments, 78(3), 031101*. doi:10.1063/1.2709758

(4)   Tamura, M., Shukuri, S., Moniwa, M., & Default, M. (1986). *Focused ion beam gallium implantation into silicon. Applied Physics A Solids and Surfaces, 39(3), 183–190*. doi:10.1007/bf00620733

(5)   Dhara, S., Marceau, R. K. W., Wood, K., Dorin, T., Timokhina, I. B., & Hodgson, P. D. (2018). *Atom probe tomography data analysis procedure for precipitate and cluster identification in a Ti-Mo steel. Data in Brief, 18, 968–982*. doi:10.1016/j.dib.2018.03.094

(6)   Vincent, G. B., Proudian, A. P., & Zimmerman, J. D. (2020). *Three dimensional cluster analysis for atom probe tomography using Ripley's K-function and machine learning. Ultramicroscopy, 113151*. doi:10.1016/j.ultramic.2020.113151.

(7)   Kühbach, M., Breen, A., Herbig, M., & Gault, B. (2019). *Building a Library of Simulated Atom Probe Data for Different Crystal Structures and Tip Orientations Using TAPSim. Microscopy and Microanalysis, 1–11*. doi:10.1017/s1431927618016252

(8)   Knipling, K. E., Narayana, P. U., & Nguyen, L. T. (2017). *Microstructures and Properties of As-Cast AlCrFeMnV, AlCrFeTiV, and AlCrMnTiV High Entropy Alloys. Microscopy and Microanalysis, 23(S1), 702–703*. doi:10.1017/s1431927617004172

(9)   Perea, D. E., Liu, J., Bartrand, J., Dicken, Q., Thevuthasan, S. T., Browning, N. D., & Evans, J. E. (2016). *Atom Probe Tomographic Mapping Directly Reveals the Atomic Distribution of Phosphorus in Resin Embedded Ferritin. Scientific Reports, 6(1).* doi:10.1038/srep22321

(10)   Hellman, O. C., & Seidman, D. N. (2002). *Measurement of the Gibbsian interfacial excess of solute at an interface of arbitrary geometry using three-dimensional atom probe microscopy. Materials Science and Engineering: A, 327(1), 24–28*. doi:10.1016/s0921-5093(01)01885-8

(11)   Krakauer, B. W., & Seidman, D. N. (1993). *Absolute atomic-scale measurements of the Gibbsian interfacial excess of solute at internal interfaces. Physical Review B, 48(9), 6724–6727*. doi:10.1103/physrevb.48.6724